J Math Chem (2008) 44:88–120
DOI 10.1007/s10910-007-9295-x

Approximate symmetry-breaking in the independent particle model of monocyclic completely conjugated polyenes

Josef Paldus · Gabriela Thiamová

Received: 18 May 2007 / Accepted: 30 July 2007 / Published online: 21 September 2007

Abstract We examine the singlet stability of symmetry adapted, restricted Hartree-Fock (RHF) solutions and the implied symmetry breaking for various planar, π-electron systems with conjugated double bonds as described by the semiempirical Pariser-Parr-Pople Hamiltonian. In particular, we explore the energy and charge-density waves (CDWs) in various real and hypothetical structures that result by a systematic deformation of the nuclear framework: we start with a highly symmetric cyclic polyene C_NH_N having a nondegenerate ground state ($N = 2n = 4\nu + 2$, $\nu = 1, 2, \ldots$), whose sites form a regular N-gon (D_{Nh} point group), and proceed to structures with lower symmetry (D_{6h}, D_{3h}, D_{2h} point groups), or with only the planar symmetry of the conjugated π-electron system (C_{1h}). The objective of this study is to explore the phenomenon that could be referred to as a breaking of an *approximate symmetry* or an *implied symmetry breaking*.

Keywords Independent particle model · Hartree-Fock equations · singlet and triplet stability · Pariser-Parr-Pople Hamiltonian · Planar conjugated systems · Cyclic polyenes

1 Introduction

Ever since the molecular orbital (MO) theory eclipsed the valence bond (VB) approach, thanks to its easier implementation in actual applications, and in spite of many desirable

J. Paldus · G. Thiamová
Department of Applied Mathematics, University of Waterloo, Waterloo, ON, Canada N2L 3G1

J. Paldus (✉)
Department of Chemistry, and Guelph-Waterloo Center for Graduate Work in Chemistry – Waterloo Campus, University of Waterloo, Waterloo, ON, Canada N2L 3G1
e-mail: paldus@scienide.uwaterloo.ca

properties of the latter (see, e.g., [1]), the Hartree-Fock (HF) approximation became the most often exploited standard tool in the exploration of the molecular (and atomic [2]) electronic structure, and became almost synonymous with the more general concept of the independent particle model (IPM). Moreover, the HF approximation represents the point of departure for most post-HF correlated methods.

The main reason for the precedence of the HF approach over other methods exploiting a single, antisymmetrized-product wave function that characterizes the IPM stems from the fact that it represents "the best" IPM from the total energy viewpoint, as well as due to the fact that the HF energy and wave function can be obtained as a solution of HF equations. These equations represent the necessary and sufficient condition for the vanishing of the first variation $\delta^{(1)}E(\Phi)$ of the mean energy functional

$$E(\Phi) = \langle\Phi|H|\Phi\rangle/\langle\Phi|\Phi\rangle, \tag{1}$$

within the manifold of the IPM wave functions $|\Phi\rangle$,

$$\Phi = (1/\sqrt{N!})\det\|\psi_1\psi_2\cdots\psi_N\|, \tag{2}$$

where ψ_i designate the orthonormal molecular spin-orbitals (MSOs).

In general, the HF equations have the form of a pseudo-eigenvalue problem,

$$F(\{\psi_j\})\psi_i = \epsilon_i\psi_i, \tag{3}$$

with $F(\{\psi_j\})$ representing an integro-differential operator, which replaces the two-body interelectronic interactions in the Hamiltonian H by an average one-electron potential due to the remaining electrons. Since these equations, in their full generality, are difficult to solve (except, possibly, for highly symmetric systems, such as atoms [2] or diatomics, when their dimensionality can be reduced to one or two spatial dimensions enabling a numerical integration), one employs the LCAO (linear combination of atomic orbitals) approximation to convert the integro-differential Eq. 3 into a finite-dimensional algebraic problem by expanding the MSOs, or corresponding molecular orbitals (MOs), in terms of a finite basis set of nonorthogonal atomic spin-orbitals (ASOs), or AOs, that define a chosen ab initio model (see Sect. 2).

The mean energy hypersurface $E(\Phi)$, Eq. 1, defined on a manifold of admissible IPM wave functions Φ, may possess, in general, a multitude of stationary points, in which the first variation $\delta^{(1)}E(\Phi)$ vanishes, and which are associated with various HF solutions. Clearly, the desired ground state solution should be associated with the absolute minimum on this hypersurface. However, the vanishing of $\delta^{(1)}E(\Phi)$ only guarantees that the solution corresponds to a stationary point, since HF Eq. 3 represent a necessary—but not a sufficient—condition for Φ to correspond to even a local minimum, not to mention the global one. The self-consistent field (SCF) iterative procedure that is generally employed when solving HF Eq. 3 will likely lead to a minimum or a saddle point that is associated with the catchment region in which lies the chosen initial or starting wave function. In this way one can often find different HF solutions in an ad hoc manner. A systematic procedure for finding all HF solutions was first presented by Kowalski and Jankowski [3]. However, such an algorithm (even at the

LCAO level) is not easy to carry out, except for simple model systems studied by these authors.

We must also keep in mind that the number and character of HF solutions will depend on the manifold of allowed IPM wave functions. When the Hamiltonian H, characterizing a given problem, possesses various symmetries that form a group $\mathcal{G}$, so that $[H, g] = 0$, $\forall g \in \mathcal{G}$, one usually restricts the IPM manifold to those wave functions that belong to the same symmetry as H [or, better, to those that transform according to the irreducible representations (irreps) of $\mathcal{G}$]. Such solutions are referred to as restricted or RHF solutions. In general, $\mathcal{G}$ is given by a direct product of subgroups that are associated with various invariant properties of the system, such as the total particle number, time reversal, spin, spatial, and other symmetries.

For molecular systems, typical symmetries of H arise from its spin independence and from the spatial symmetry of the frozen nuclear framework that defines the electronic Hamiltonian in the Born–Oppenheimer approximation. Thus, for an $N = 2n$ electron closed-shell molecular system, the RHF wave function Φ has the form of a pure-singlet Slater determinant with doubly occupied spatial MOs ϕ_i that transform according to the irreps of a relevant point group, namely

$$\Phi = (1/\sqrt{(2n)!}) \det\|\phi_1\alpha, \phi_1\beta, \phi_2\alpha, \phi_2\beta, \ldots, \phi_n\alpha, \phi_n\beta\| \,. \tag{4}$$

When we require that all degenerate MOs are either doubly occupied or unoccupied, Φ will belong to the totally symmetric irrep of a given point group, and will be referred to as a symmetry-adapted (SA) RHF solution. In an open-shell case, one employs a restricted open-shell HF (ROHF) IPM wave function that is associated with a high-spin component for a given spin-multiplet and is represented by a determinant with a doubly occupied core and an open-shell part consisting of MOs having the same spin.

Now, if we restrict our variational manifold to SA wave functions that constitute simultaneous eigenstates of H and all of $g \in \mathcal{G}$, we are in fact imposing constraints on the variational problem for $E(\Phi)$, Eq. 1. These constraints reduce the most general IPM manifold to the corresponding SA submanifold, and thus can only raise the variational energy. This fact is the essence of the so-called "symmetry dilemma" of Löwdin [4], since by allowing broken symmetry (BS) solutions we can improve the upper bound to the energy. Thus, loosely speaking, by allowing an a priori "lousy" wave function, we can obtain, at least in principle, a better upper bound for the energy.

In actual applications it is usually the spin symmetry that is given up, since it proved to be the most effective in the energy lowering of the SA solution, as long as a BS solution with lower energy exists. This is usually the case for structures involving highly stretched chemical bonds or for electron-rich systems. The simplest way to break the spin symmetry is to employ different orbitals for different spins (DODS) wave function, displaying a nonvanishing spin-density waves (SDWs). A more sophisticated breaking of spin symmetry may involve torsional spin-waves, or we may even break the S_z symmetry by considering general spin functions, as given by a general linear combination of the α and β spins (for detailed classification of BS solutions, see [5–7]). Such DODS BS solutions may often be found even for closed-shell molecules, and were first generated by Koutecký [8]. While in the closed-shell case such

DODS solutions are found only in special circumstances, they are invariably present for open-shell systems.

A methodical characterization of HF solutions in terms of their stability was initiated by Thouless [9], who considered the second variation $\delta^{(2)}E(\Phi)$ of the mean energy functional 1 and formulated general stability conditions. Clearly, if a given HF solution is to correspond to a (local or global) minimum on $E(\Phi)$, its second variation must be positive definite, i.e., $\delta^{(2)}E(\Phi) > 0$. Since $\delta^{(2)}E(\Phi)$ can be represented as a quadratic form in terms of variational parameters, the stability conditions may be characterized by the associated eigenvalue problem. Thus, for a solution to be stable, all eigenvalues of the stability problem must be positive, while the presence of one or more negative eigenvalues implies the instability, the corresponding stationary point having the character of a saddle point. Moreover, the eigenvector associated with the smallest negative eigenvalue gives the direction of the steepest descent on $E(\Phi)$ at the stationary point [6,10,11].

For a spin-independent electronic Hamiltonian describing a closed-shell system (cf. Eq. 4), the Thouless stability conditions may be factorized into the four subproblems [10], three of which are identical and can be associated with the spin-symmetry breaking, while the remaining one preserves the spin symmetry and leads to the breakdown of spatial (and/or some other, e.g., alternancy [12]) symmetry. The corresponding instabilities were referred to by Čížek and Paldus [10,11] as the *triplet* (or non-singlet) and *singlet* ones, respectively. The triplet instability leads to an unrestricted HF (UHF) solution of the DODS type with a SDW, while the singlet instability implies the existence of a pure-singlet, BS solution with doubly occupied MOs that is characterized by various types of charge-density waves (CDWs). The existence of such solutions was amply demonstrated in several studies using semiempirical Hamiltonians [10,13–15], and later on for the standard ab initio model Hamiltonians (see, e.g., [16–20]; for an overview see [7] and Sects. 3.6–3.8 of [6]). A similar development was carried out concerning the stability of the ROHF solutions for simple open-shell systems [21–25] (see also [6,7]), as well as for Brueckner (or maximum overlap) IPM wave functions [26].

The primary goal of this paper is to examine the singlet stability conditions, and the nature of the resulting BS solutions, for a number of real, as well as hypothetical, π-electron model systems, having different spatial symmetry and nuclear-framework geometry, in order to better understand the appearence and properties of the resulting SA and BS solutions. We employ a semiempirical model Hamiltonian of the Pariser-Parr-Pople (PPP) type [27], and our model systems represent various planar, π-electron networks with conjugated double bonds, ranging from the most symmetric cyclic polyenes C_NH_N with a nondegenerate ground state ($N = 2n = 4\nu + 2$; the so-called Hückel rule), to their various stereoisomers with lower symmetry, primarily the "perimeter models" of corresponding polycyclic aromatic hydrocarbons. Such monocyclic, completely conjugated hydrocarbons are generally referred to as [N]annulenes. Since, however, this term is normally associated with the most stable conformer, invariably represented by a "perimeter model" or p-model of some polycyclic aromatic hydrocarbon, we prefer the p-model terminology so that we can easily distinguish different stereoisomers (see Sects. 5, 7, and 8 for more detail).

In order to introduce the necessary notation, we first recall the matrix form of HF equations and of the corresponding singlet and triplet stability conditions for the closed-shell case. We then define the model Hamiltonian employed and present the results and their discussion.

2 Hartree-Fock-Roothaan equations [28]

The algebraic form of HF Eq. 3 in their LCAO form is usually referred to as the Hartree-Fock-Roothaan (HFR) equations. One thus approximates each orthonormal molecular spin-orbital (MSO) ψ_i by a linear combination of a finite set of nonorthogonal (but normalized) atomic spin-orbitals (ASOs) χ_μ, $(\mu = 1, \ldots, m)$

$$\psi_i = \sum_{\mu=1}^{m} C_{\mu i}\chi_\mu, \qquad \langle\psi_i|\psi_j\rangle = \delta_{ij}, \qquad \langle\chi_\mu|\chi_\nu\rangle = S_{\mu\nu}, \qquad S_{\mu\mu} = 1. \tag{5}$$

Introducing row matrices of ASOs and MSOs by

$$\boldsymbol{\chi} = \|\chi_1 \cdots \chi_m\|, \qquad \boldsymbol{\psi} = \|\psi_1 \cdots \psi_N\|, \tag{6}$$

we can write the first Eq. 5 as

$$\psi_i = \boldsymbol{\chi}\mathbf{c}_i, \qquad \mathbf{c}_i^T = \|C_{1i}C_{2i}\cdots C_{mi}\|, \tag{7}$$

where $\mathbf{c}_i$ is a column vector and $\mathbf{c}_i^T$ designates its transpose, or globally as

$$\boldsymbol{\psi} = \boldsymbol{\chi}\mathbf{C}, \qquad \mathbf{C} = \|C_{\mu i}\|_{m\times N} = \|\mathbf{c}_1\mathbf{c}_2\cdots\mathbf{c}_N\|. \tag{8}$$

In a closed-shell case, HF equations will generate m MOs, $(m \geqslant N)$, of which only $n = N/2$ will be doubly occupied. Using a minimum AO basis set, we have in fact $m = N = 2n$, so that only half of the MOs that are generated is doubly occupied, the remaining ones forming the virtual MOs. The canonical version of HFR equations then takes the form [28]

$$\mathbf{F}(\{\mathbf{c}_j\})\mathbf{c}_i = \epsilon_i\mathbf{S}\mathbf{c}_i \qquad \text{or} \qquad \mathbf{F}(\{\mathbf{C}_{\text{occ}}\}) = \mathbf{S}\mathbf{C}\boldsymbol{\epsilon}, \tag{9}$$

where $\boldsymbol{\epsilon} = \|\epsilon_i\delta_{ij}\|$ is a diagonal matrix of orbital energies.

The Fock operator $\mathbf{F} = \|F_{\mu\nu}\|$ has the general form

$$F_{\mu\nu} = h_{\mu\nu} + \sum_{j\,(\text{occ})} \langle\mu j|v|\nu j\rangle_A, \tag{10}$$

with $h_{\mu\nu}$ designating the one-electron component of H, and $\langle\mu j|v|\nu j\rangle_A$ the antisymmetrized two-electron integral defined as

$$\langle\mu j|v|\nu j\rangle_A = \langle\mu j|v|\nu j\rangle - \langle\mu j|v|j\nu\rangle, \qquad \langle\mu j|v|\nu j\rangle \equiv \langle\chi_\mu\psi_j|v|\chi_\nu\psi_j\rangle. \tag{11}$$

In the closed-shell case, with Φ given by Eq. 4, we then have

$$F_{\mu\nu} = h_{\mu\nu} + \tfrac{1}{2}\sum_{\lambda\kappa} p_{\lambda\kappa}\langle\mu\lambda|v|\nu\kappa\rangle_a, \tag{12}$$

where now

$$\langle\mu\lambda|v|\nu\kappa\rangle_a = 2\,\langle\mu\lambda|v|\nu\kappa\rangle - \langle\mu\lambda|v|\kappa\nu\rangle, \tag{13}$$

and $p_{\mu\nu}$ designates the element of the first order density matrix $\mathbf{P}$,

$$\mathbf{P} = \|p_{\mu\nu}\|, \qquad p_{\mu\nu} = 2\sum_{i=1}^{n} \bar{C}_{\mu i} C_{\nu i}, \tag{14}$$

where the sum extends over the occupied MOs.

3 Stability conditions

An arbitrary IPM wave function Φ that is not orthogonal to a HF or HFR wave function Φ_0, and thus lies in the "neighborhood" of Φ_0, may be expressed, according to Thouless' theorem [9], in the form

$$|\Phi\rangle = \exp(\hat{D})|\Phi_0\rangle, \tag{15}$$

where the operator $\hat{D}$

$$\hat{D} = \sum_{a,r}\sum_{\sigma,\tau=\alpha,\beta} d_{a\sigma}^{r\tau}\,\hat{X}_{r\tau}^{\dagger}\hat{X}_{a\sigma} = \sum_{A,R} d_A^R\,\hat{X}_R^{\dagger}\hat{X}_A, \tag{16}$$

represents all possible monoexcitations promoting an occupied spin-orbital $a\sigma \equiv |a\rangle|\sigma\rangle \equiv |A\rangle \equiv A$ to a virtual one $r\tau \equiv |r\rangle|\tau\rangle \equiv |R\rangle \equiv R$. Here, and in the following text, $\hat{X}_I^{\dagger}$ and $\hat{X}_I$ designate fermionic creation and annihilation operators associated with the spin-orbital basis $\{|I\rangle\}$. We will employ generic labels $A, B, \ldots$ for the occupied spin-orbitals and $R, S, \ldots$ for the virtual ones, and arrange the variational coefficients d_A^R into a column matrix $\mathbf{D}$ in some a priori fixed order, e.g.,

$$\mathbf{D}^T = \|d_A^R d_A^S \cdots d_B^R d_B^S \cdots\|\,. \tag{17}$$

The second variation $\delta^{(2)}E(\Phi_0)$ can then be expressed as a quadratic form [9,10]

$$\delta^{(2)}E(\Phi_0) = \mathbf{X}^{\dagger}\mathbf{W}\mathbf{X}, \qquad \mathbf{X} = \begin{Vmatrix}\mathbf{D}\\ \bar{\mathbf{D}}\end{Vmatrix}, \qquad \mathbf{W} = \begin{Vmatrix}\mathbf{A} & \mathbf{B}\\ \bar{\mathbf{B}} & \bar{\mathbf{A}}\end{Vmatrix}, \tag{18}$$

where the square matrices **A** and **B** have the elements

$$(\mathbf{A})_{AB}^{RS} = f_{RS}\delta_{AB} - f_{AB}\delta_{RS} + \langle RB|v|AS\rangle_A,$$
$$(\mathbf{B})_{AB}^{RS} = \langle AB|v|RS\rangle_A, \tag{19}$$

so that **W** is Hermitian since $\mathbf{A}^\dagger = \mathbf{A}$ and $\mathbf{B}^\dagger = \bar{\mathbf{B}}$, a bar designating complex conjugation.

Thus, for $\delta^{(2)}E(\Phi_0)$ to be positive definite, it is necessary and sufficient that all the eigenvalues λ_i of **W**,

$$\mathbf{W}\mathbf{Y}_i = \lambda_i \mathbf{Y}_i, \qquad \mathbf{Y}_i = \begin{Vmatrix} \mathbf{Z}_i \\ \bar{\mathbf{Z}}_i \end{Vmatrix}, \tag{20}$$

be positive. In most actual applications **A** and **B** are real, in which case the eigenvalue problem 20 can be factorized into the two subproblems [10]

$$(\mathbf{A} \pm \mathbf{B})\mathbf{Z}_i^{(\pm)} = \lambda_i^{(\pm)}\mathbf{Z}_i^{(\pm)}, \tag{21}$$

where $\mathbf{Z}_i^{(\pm)} = \mathbf{Z}_i \pm \bar{\mathbf{Z}}_i$. Thus, if at least one of the eigenvalues λ_i is negative, i.e., $\lambda_1 < 0$, the HF solution Φ_0 does not represent a local minimum within the variational space considered, and the corresponding eigenvector $\mathbf{Z}_1$ gives a direction of the steepest descent on the hypersurface $E(\Phi)$, Eq. 1, at $\Phi = \Phi_0$ (see [6] for details).

4 Singlet and triplet stability conditions

For a spin-independent Hamiltonian H that commutes with both $\hat{S}_z$ and $\hat{S}^2$, the HF stability conditions in their general spin-orbital form can be further factorized into the singlet and triplet (or, more correctly, nonsinglet) stability conditions [10]. The closed-shell type IPM wave function 4 automatically preserves the $\hat{S}_z$ component of total spin, as does the corresponding UHF wave function. Thus, in this case, only the total spin symmetry can be violated. As shown in detail in references [10,22] or [6], the general spin-orbital stability conditions 20 or 21 factorize in this case into what we refer to as the *singlet* and *triplet* stability conditions, characterized by matrices $\mathbf{A}^{s,t}$ and $\mathbf{B}^{s,t}$ with matrix elements

$$(\mathbf{A}^{s,t})_{ab}^{rs} = \langle r|f|s\rangle\delta_{ab} - \langle b|f|a\rangle\delta_{rs} + 2\xi\langle rb|v|as\rangle - \langle rb|v|sa\rangle,$$
$$(\mathbf{B}^{s,t})_{ab}^{rs} = 2\xi\langle ab|v|rs\rangle - \langle ab|v|sr\rangle, \tag{22}$$

where $\xi = 1$ in the singlet case and $\xi = 0$ in the triplet case, while the lower case letters designate spin-independent MOs, i.e., a designates ϕ_a, $(a = 1, 2, \ldots, n)$ and similarly for virtual orbitals.

The singlet and nonsinglet (triplet) instabilities, as implied by the sign of the lowest root of the respective stability problem, represent the most surprising instabilities for closed-shell systems. The occurrence of a triplet instability that implies the existence

of an UHF solution of the DODS type with lower energy than the spin-symmetry adapted RHF solution, is very common, and is invariably found when breaking true chemical bonds, since the RHF potential energy curve, or surface, leads to wrong dissociation products. However, the presence of a singlet instability is much more intriguing, since it implies the existence of another pure-singlet RHF solution. Such solutions generally break the spatial symmetry, as characterized by the point group of the frozen nuclear framework of the electronic Hamiltonian.

The energy lowering associated with these singlet BS solutions is generally much smaller than is the case for UHF solutions. Although an unambiguous interpretation of the physical or chemical meaning of such BS solutions is not easy to establish (cf., e.g., Refs. [6,29] and [30]), and their existence may be simply an expression of the fact that the HF approximation is inadequate in a given case, there is nonetheless a definite evidence that in some cases such an instability suggests a preferred distortion of the nuclear framework. This is the case, for example, for polyenic chains, as modeled by cyclic polyenes [31], or for other electron-rich systems (see [6]), where the actual symmetry breaking of the nuclear framework persists even at the correlated level (see, e.g., Refs. [31–40]).

In the case of atoms, the breaking of spherical symmetry indicates a tendency to autoionization or, simply, a physical instability of a given system [18,41]. For molecular systems, the existence of a BS RHF solution due to a singlet instability implies a nuclear framework distorsion at the HF level of approximation, since it can be shown [6] that lowering of the symmetry of the nuclear framework, as implied by the BS solution and its CDW, leads to an energy lowering at the HF level (see Sect. 3.3 of [6]). Of course, this distortion may or may not persist at the correlated level. For this very reason we have decided to focus in this work on a study of the occurrence of singlet instabilities and the character of implied BS solutions for various hypothetical structures that will enable us to pursue this phenomenon at various stages of the nuclear framework distortion, as will be explained below.

5 Model description

5.1 Pariser-Parr-Pople (PPP) Hamiltonian [27]

We investigate various, mostly hypothetical, planar π-electron systems with conjugated double bonds as described by the Pariser-Parr-Pople Hamiltonian [27,42]

$$H_{\mathrm{PPP}} = \sum_{\mu} \alpha_{\mu} + \sum_{\mu,\nu}{}' \beta_{\mu\nu} E_{\mu\nu} + \sum_{\mu<\nu} \gamma_{\mu\nu} (E_{\mu\mu} - Z_{\mu})(E_{\nu\nu} - Z_{\nu}) + \tfrac{1}{2} \sum_{\mu} \gamma_{\mu\mu} E_{\mu\mu} (E_{\mu\mu} - 1), \tag{23}$$

where the prime on the second summation symbol implies the tight-binding approximation (sum extends only over nearest neighbors), α_{μ} and $\beta_{\mu\nu}$ are the so-called Coulomb and resonance (or hopping) one-electron integrals, $\gamma_{\mu\nu} \equiv \langle \mu\nu | v | \mu\nu \rangle$ is the two-electron Coulomb integral, and Z_{μ} is the number of π-electrons contributed by

the μ-th atomic site (see, e.g., Sect. VI.C.2 of [42]). The unitary group generators [42] $E_{\mu\nu}$,

$$E_{\mu\nu} = \sum_{\sigma=\pm 1/2} X^{\dagger}_{\mu\sigma} X_{\nu\sigma}, \tag{24}$$

are defined in a hypothetical basis of symmetrically orthogonalized $2p_z$ carbon atomic spin-orbitals $|\mu\sigma\rangle = |\mu\rangle|\sigma\rangle$, $\sigma = \pm\frac{1}{2}$.

For neutral, unsaturated hydrocarbons with conjugated double bonds, in which each atomic site contributes only one electron ($Z_\mu = 1$), we can assume that all one-center integrals are identical, namely $\alpha_\mu \equiv \alpha$ and $\gamma_{\mu\mu} \equiv \gamma_{11}$, and without any loss of generality set $\alpha = 0$, obtaining a simplified form of the PPP Hamiltonian 23,

$$\tilde{H}_{\mathrm{PPP}} = \sum_{\mu,\nu}{}' \beta_{\mu\nu} E_{\mu\nu} + \tfrac{1}{2} \sum_{\mu,\nu} \gamma_{\mu\nu} (E_{\mu\mu} - 1)(E_{\nu\nu} - 1). \tag{25}$$

Moreover, when all the C–C bondlengths are assumed to be identical, we can also set $\beta_{\mu\nu} = \beta$. Thus, the only semiempirical parameters that specify this simplified PPP Hamiltonian $\tilde{H}_{\mathrm{PPP}}$ are the resonance integral β, whose spectroscopic value is usually set equal to $-2.4\,\mathrm{eV}$, and the two-electron Coulomb integrals $\gamma_{\mu\nu}$ that are evaluated according to various approximations (see [27]). Here we employ a simple Mataga-Nishimoto [43] approximation, which approximates the two-electron integrals $\gamma_{\mu\nu}$ via a simple Coulomb interaction between the two point charges located at sites μ and ν, which is modified in such a way so as to obtain the on-site self-interaction integral γ_{11}, given by the difference of the valence state ionization potential I and the electron affinity A for the $2p_z$ carbon atomic orbital (the so-called I–A approximation of Goeppert-Mayer and Sklar [44]). Taking the γ_{11} value to be equal to 10.84 eV, we thus have

$$\gamma_{\mu\nu} = e^2/(R_{\mu\nu} + a), \qquad \gamma_{11} = e^2/a = 10.84\,\mathrm{eV}. \tag{26}$$

We note that the PPP Hamiltonian represents a generalization of the Hubbard Hamiltonian that is often used in solid-state physics and in which only the on-site Coulomb interactions are taken into account, i.e., $\gamma_{\mu\nu} = \gamma_{11}\delta_{\mu\nu}$. The advantage of the Hubbard Hamiltonian is the fact that it involves only two parameters characterizing, respectively, the one- and two-electron interactions, namely the hopping integral $\beta \equiv -t$ and the on-site interelectronic repulsion $\gamma_{11} \equiv U$. This makes it possible to derive exact results for highly symmetric systems, such as cyclic polyenes $C_N H_N$, even when $N \to \infty$, by solving the so-called Lieb-Wu equations [45], as well as to examine the studied systems in the whole range of the correlation regime [46,47] as a function of the coupling constant (U/t). Although the PPP Hamiltonian treats the interelectronic interaction in a more realistic way, we can still explore the behavior of the studied systems in the whole range of the coupling constant by keeping the $\gamma_{\mu\nu}$ integrals at their standard values, while changing β. Then the coupling constant is proportional to $1/\beta$, with $\beta = 0$ characterizing the fully correlated limit and $|\beta| \to \infty$ the uncorrelated limit (in practice achieved at $|\beta| \sim 5\,\mathrm{eV}$). Clearly, the latter limit is equivalent to the

Hückel approximation, while in the fully correlated limit ($\beta = 0$), each VB structure provides the exact HF solution (see below).

5.2 Model systems

We employ planar, π-electron networks with conjugated double bonds to explore the singlet stability of SA RHF solutions and, in the presence of an instability, we investigate the implied closed-shell, pure-singlet BS RHF solutions. The objective of this exercise is to explore the occurrence and character of BS solutions, of their energies relative to the SA ones, as well as the role of the point group symmetry of the underlying nuclear framework, on the propagation of these solutions and of the associated CDWs to systems with a lower symmetry, or no spatial symmetry at all, namely the phenomenon that could be referred to as a breaking of an "approximate symmetry" or an"induced" symmetry breaking.

For this reason, we examine these solutions in the whole range of the coupling constant or, equivalently, of its inverse given by the value of the resonance integral β. We start with the most symmetric structures having $N = 2n = 4\nu + 2$ sites and a nondegenerate ground state, as represented by the cyclic polyenes C_NH_N, which possess the D_{Nh} symmetry of a regular N-gon. In this case, the RHF solution is in fact completely determined by the symmetry of the system in any minimum basis set, whether semiempirical or ab initio, and the RHF MOs are identical with either the Hückel or Brueckner (maximum overlap) MOs for any value of the coupling constant. The singlet stability of these solutions was explored in detail in our earlier studies [10,15,14,31], as well as the implied BS solutions, which display either the diagonal or the off-diagonal CDWs (see also [48]). The former ones break both the spatial and the alternancy symmetries (their CDWs are formed by the alternating atomic charges $p_{\mu\mu}$), and are again singlet unstable, while those that are associated with the off-diagonal CDWs (represented by the alternating bond-orders $p_{\mu\nu}$) are singlet stable. For $N \to \infty$ these systems model linear polyenic chains with Born–von Kármán boundary conditions and imply the existence of the bond-length alternation that persists even when higher-order correlated methods are employed [31–36,49,50].

Starting with these highly symmetric structures, we then gradually lower the D_{Nh} symmetry by distorting the nuclear framework so that it fits with the perimeter of some polycyclic aromatic hydrocarbon, unless otherwise stated (in which case we explicitly specify the geometry of the nuclear framework employed). We then refer to these distorted systems as "perimeter models" or p-models of a given polycyclic hydrocarbon. In forming the p-models, we keep all the C–C bond lengths constant and equal to 1.4 Å and the C–C–C angles equal to $2\pi/3$. For example, the $N = 10$ cyclic polyene eventually becomes the p-naphthalene, $N = 14$ cyclic polyene the p-anthracene or p-phenanthren, etc. (see Fig. 1), i.e., systems with the D_{2h} or C_{2v} symmetry. For larger cycles, we can also arrive to p-models of other polycyclic hydrocarbons, including those having the hexagonal or trigonal symmetry, or even to completely asymmetric structures, such as p-benzanthracene.

Wherever our p-models describe actually existing systems that were synthetized and studied experimentally (for reviews see references [51–53] and monographs [54,55]),

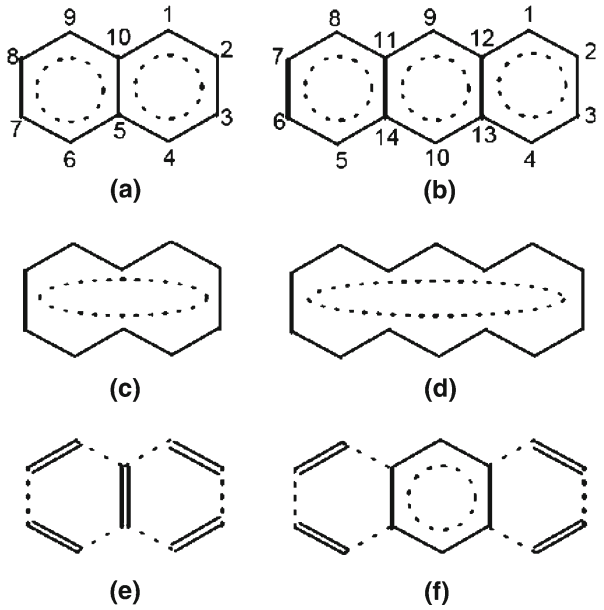

Fig. 1 The linear polyacenes naphtalene (**a**) and anthracene (**b**), and their cyclic polyene "perimeter" versions p-naphtalene (**c**) and p-anthracene (**d**). The structures (**e**) and (**f**) describe corresponding symmetry-adapted RHF solutions in the fully correlated limit ($\beta = 0$). For structures (**a**) and (**b**) we also indicate the site-numbering used for all these systems. See the text for details

we also provide the approprite terminology that is used by organic chemists. These completely conjugated, monocyclic polyenes are generally referred to as $[N]$annulenes. They indeed have a more or less developed aromatic character when N satisfies the Hückel $(4\nu + 2)$ rule, while those with 4ν carbon sites are non- or even antiaromatic. They generally possess the structure that avoids as much as possible the steric effects or their planarity is stabilized with transannular bridges (see Sect. 7).

When interpreting our results, we will also find useful some basic theorems concerning the existence of BS solutions for hydrocarbons with conjugated double bonds. We recall them in the next section.

6 Some basic theorems

We next recall the basic theorem concerning the singlet stability of the RHF solutions for planar conjugated systems in the fully correlated limit, as well as its important corollary. These theorems were formulated in our earlier study [13] of the singlet stability and of the corresponding BS RHF solutions for polycyclic, alternant hydrocarbons, and are based on the properties of RHF solutions in the fully correlated limit ($\beta = 0$). They will help us to understand some of our results and we thus recall their essence below.

Theorem 6.1 *[13] For $\beta = 0$, any Kekulé or Dewar structure represents the exact RHF solution Φ_0, Eq. 4, with ethylene-like MOs ϕ_i of the general form*

$$\phi_i = (\chi_\mu + \chi_\nu)/\sqrt{2}, \tag{27}$$

where μ and ν designate the sites forming a bond (for Kekulé structures, μ and ν represent nearest neighbors). The total π-electron energy of such a solution is given by the sum of ethylene-like orbital energies $\epsilon_i^- = \frac{1}{2}(\gamma_{11} - \gamma_{\mu\nu})$. Thus, the Dewar-type solutions have higher energy than the Kekulé ones, the latter having the same total π-electron energy equal to $E_0(\beta = 0) = n(\gamma_{11} - \gamma_{12})/2$. For alternant systems this energy represents the absolute minimum on the mean energy hypersurface $E(\Phi)$, Eq. 1, on the manifold of IPM wave functions 4.

From the fact that at $\beta = 0$, Kekulé solutions correspond to the absolute minimum on the mean energy hypersurface $E(\Phi)$, Eq. 1, and the fact that the one-electron part of the Hamiltonian can only further stabilize such solutions, we can conclude the followings rule for the stability of HF solutions of the studied systems:

Corollary 6.2 *[13] Let the invariance group of the Hamiltonian (i.e., of the nuclear framework) of our system be the point group $\mathcal{G}$. When there exists a Kekulé structure having the same invariance group $\mathcal{G}$, then the SA RHF solution is always singlet stable. However, when all possible Kekulé structures possess the symmetry of some nontrivial subgroup $\mathcal{G}'$ of $\mathcal{G}$, i.e., $\mathcal{G}' \subsetneqq \mathcal{G}$, then the SA RHF solution may become singlet unstable for some β in the interval $0 \leqslant \beta < \beta_{\text{crit}}$, β_{crit} representing the critical β value for the onset of instability.*

7 Results and discussion

As is well known [10,31], the SA RHF solution for cyclic polyenes C_NH_N becomes singlet unstable as we approach the fully correlated limit. The absolute value of the critical resonance integral β_{crit} increases with increasing N (cf. Fig. 2 and [31]). Thus, while for $N = 6$ (benzene) $|\beta_{\text{crit}}|$ amounts to only $\sim$0.3 eV, it exceeds the spectroscopic value of $|\beta|$ already for $N = 26$ (or $\nu = 6$). We recall here that, in contrast, there is only a slight dependence of $|\beta_{\text{crit}}|$ on the size of linear polyacenes, as measured by their number of sites N or the number of the benzene rings ν (cf. Fig. 2 and [13]). Moreover, the SA RHF solutions for polyacenes with an even number of benzene rings are always singlet stable, since they possess a fully symmetric D_{2h} Kekulé structure [13] (cf. Corollary 6.2). Considering the p-models of these polyacenes (Fig. 2), we find again a significant dependence of $|\beta_{\text{crit}}|$ on N, even though less pronounced than for the D_{Nh} cyclic polyenes C_NH_N. Of course, all these three types of systems coincide for $N = 6$ or $\nu = 1$. It will thus be of interest to examine the behaviour of SA and, whenever they exist, of BS solutions and their energies, in the whole range of the coupling constant, proceeding from the D_{Nh} structures to various deformed D_{2h} or even completely asymmetric ones.

For $|\beta| < |\beta_{\text{crit}}|$ we can thus generate BS RHF solutions with lower energy than that of the SA RHF solution. This can be most easily done by choosing a suitable bond-order

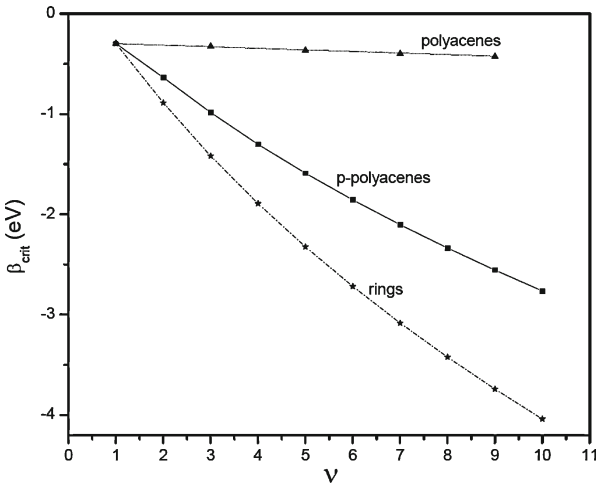

Fig. 2 The dependence of the critical β values, β_{crit}, (in eV) for linear polyacenes with ν benzene rings, their "perimeter" D_{2h} p-polyacene versions (see Fig. 1), and D_{Nh} cyclic polyenes C_NH_N, $N = 2n = 4\nu + 2$ (rings), having a nondegenerate ground state, as a function of their size measured by the parameter ν

(BO) matrix as the initial approximation in the SCF iterative process, even though in special cases more care is required (cf. [10]). As we have already noted, for sufficiently large N (or for small enough $|\beta|$ values when we fix N), we find two negative roots in the singlet stability problem for cyclic polyenes C_NH_N that lead, respectively, to diagonal (atomic charge alternating) and off-diagonal (bond-order alternating) CDW solutions. The diagonal CDW solutions are themselves singlet unstable, leading eventually to stable off-diagonal CDW solutions, representing the true RHF ground state, contrary to some earlier claims (cf. [48] vs. [56–58]). Thus, by a BS solution we shall always understand a stable BS solution.

7.1 $C_{10}H_{10}$ and $C_{14}H_{14}$ structures

Since for the smallest ring ($N = 6$) there is no difference between the cyclic polyene itself (i.e., benzene) and its p-model, namely p-benzene, we first focus our attention on the next two cases, namely on C_NH_N with $N = 10$ and 14, whose p-model versions correspond to the perimeter models of naphthalene and anthracene (Fig. 1). Only in the fully correlated limit ($\beta = 0$) the p-models coincide with the corresponding polyacenes. We recall a very different behaviour of linear polyacenes having an even or an odd number of benzene rings [13], which is reflected in the behaviour of the corresponding p-models, especially in the vicinity of the strongly correlated limit ($\beta = 0$).

We first consider the energy difference ΔE between the SA and BS solutions,

$$\Delta E = E_0^{\text{SA}} - E_0^{\text{BS}}, \tag{28}$$

which is defined and positive in the region of the instability of the SA solution, $|\beta| < |\beta_{\text{crit}}|$. For the D_{Nh} cyclic polyenes, ΔE monotonically increases with decreasing $|\beta|$ value, reaching its maximum at $\beta = 0$, as may be seen in Figs. 3 and 4 for $N = 10$ and 14, respectively. However, this behaviour, which one would expect on the first sight, does not occur in general for distorted cyclic polyenes. Indeed, when we lower the D_{Nh} symmetry of cyclic polyenes $C_N H_N$ by distorting their nuclear framework, as indicated in Fig. 3 and 4, reaching, eventually, the p-models of linear polyacenes (p-naphthalene and p-anthracene), having the point group symmetry D_{2h}, we invariably observe that once the deformation of the nuclear framework reaches certain stage, the energy difference ΔE, Eq. 28, reaches its maximum at some nonvanishing value of $|\beta|$, and then starts decreasing. In fact, for the p-naphthalene (Fig. 3), it vanishes at $\beta = 0$, while for the p-anthracene (Fig. 4) it reaches a certain finite value in the fully correlated limit.

A clue to this different behaviour may be understood when we consider the stability and BS solutions for the actual linear polyacenes, namely for naphthalene and anthracene. We know that for naphthalene, the SA solution is always stable, since there exists a Kekulé structure having the D_{2h} symmetry, while this is not the case for anthracene [13]. However, for $\beta = 0$, there is no difference between the Hamiltonians describing the actual polyacene and its p-model. Thus, ΔE for p-naphthalene must vanish at $\beta = 0$, while for p-anthracene it must coincide with that of anthracene (cf. curves 4 and 5 in Fig. 4).

Yet, focussing solely on the energy characteristics of the SA and BS solutions does not reveal the whole story. When we consider the roots of the singlet stability problem, shown in Figs. 5 and 6 for the p-naphthalene and p-anthracene, respectively,

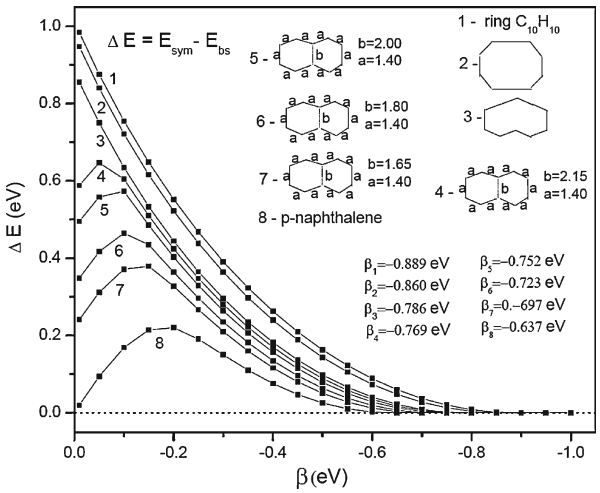

Fig. 3 The energy difference ΔE (in eV) between the symmetry-adapted (SA) and broken-symmetry (BS) RHF solutions for $C_{10}H_{10}$ cyclic polyenes, $\Delta E = E_{SA} - E_{BS}$, as a function of the resonance integral β (in eV). The individual structures range from the fully symmetric $C_{10}H_{10}$ ring with D_{10h} point group symmetry to the D_{2h} p-naphthalene and similar intermediately distorted structures as indicated in the figure. The critical β values are also listed in the figure for each case

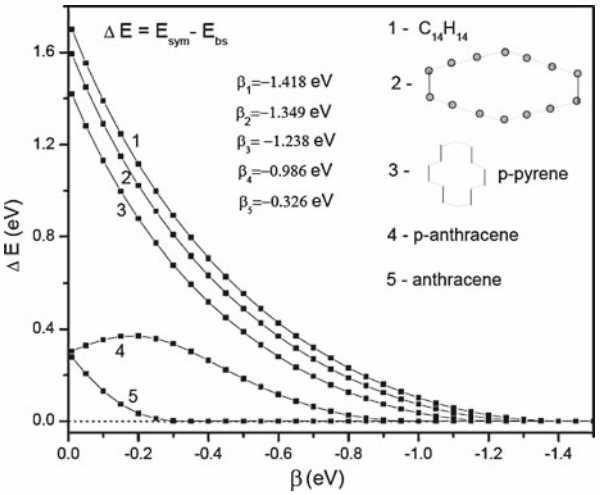

Fig. 4 The energy difference ΔE (in eV) between the symmetry-adapted (SA) and broken-symmetry (BS) RHF solutions for $C_{14}H_{14}$ cyclic polyenes, $\Delta E = E_{SA} - E_{BS}$, as a function of the resonance integral β (in eV). See Fig. 3 and the text for details

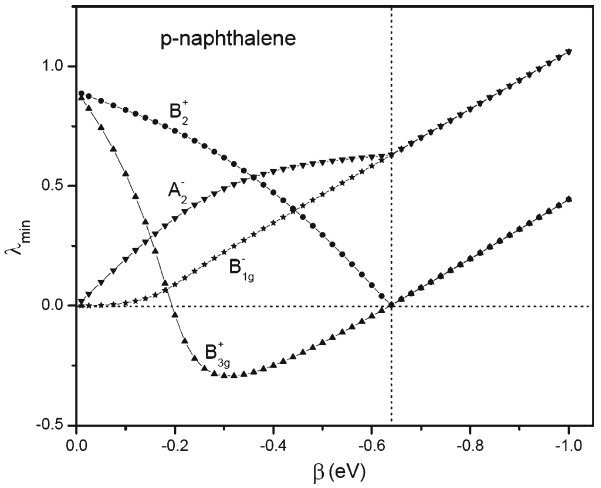

Fig. 5 The dependence of the two lowest-lying roots $\lambda_{\min}$ of the singlet stability problem for the SA (curves B_{3g}^{+} and B_{1g}^{-}) and BS (curves A_2^{-} and B_2^{+}) RHF solutions for p-naphthalene as a function of the resonance integral β (in eV). The curves are labeled by the respective irreducible representations of the D_{2h} and C_{2v} point groups, and the vertical dashed line at $\beta = -0.637$ eV indicates the critical resonance integral value

we observe that in the former case there is a region of $|\beta|$ values near $\beta = 0$, where no singlet instability is present, while in the case of p-anthracene, the singlet instability persists all the way to the fully correlated limit.

In order to understand this behaviour in the case of p-naphthalene, we examined the character of the mean-energy hypersurface $E(\Phi)$ in the neighborhood of the relevant

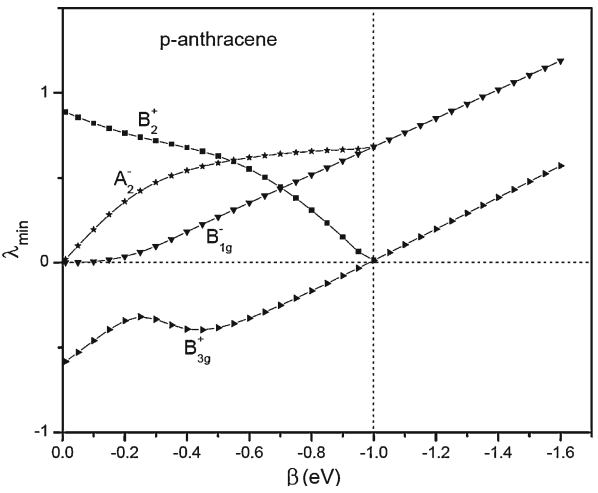

Fig. 6 Same as Fig. 5 for p-anthracene, with $\beta_{\text{crit}} = -0.986\,\text{eV}$

SA and BS solutions. The nature of this surface is schematically represented in Fig. 7 as a one-dimensional energy plot along a hypothetical coordinate in the variational manifold passing through the relevant SA and BS solutions. We know (Theorem 6.1) that at $\beta = 0$ the RHF solutions are represented by Kekulé structures, all having the same energy, and the corresponding minimum is of a higher than second order, since the second variation $\delta^{(2)}E(\Phi)$ at these solutions vanishes. When we move away from the fully correlated limit by slightly increasing the $|\beta|$ value, the SA solution remains to be stable, but its energy decreases with increasing $|\beta|$ value at a slower rate than does that of the BS solution, thus increasing the ΔE gap and, at the same time, the curvature associated with the corresponding minimum also increases (cf. Figs. 5 and 7). Eventually, around $|\beta| \sim 0.2\,\text{eV}$ this local minimum disappears, resulting in an unstable SA solution associated with a local maximum on a schematic plot in Fig. 7. With further increase of $|\beta|$, this maximum becomes less and less prominent relative to the minimum characterizing the BS solution, untill it disappears altogether at $\beta = \beta_{\text{crit}} = -0.637\,\text{eV}$.

In Fig. 7 we also indicated the overlap between the SA and BS solutions, as well as between the two degenerate BS solutions. We see that as we approach β_{crit} these overlaps steadily increase towards their maximum possible value of one, and the BS solutions merge with the now stable SA solution at $\beta = \beta_{\text{crit}}$. We should also mention the switch of the lowest root of the stability problem from the B_{3g}^+ symmetry species to B_{1g}^- in the case of p-naphthalene, while no such switching occurs for p-anthracene (cf. Figs. 5 and 6). This switch occurs due to the orbital energy crossing (at about $\beta \sim -0.3\,\text{eV}$ for the two highest occupied and the two lowest unoccupied MOs). However, this has no effect on the smoothness of the total energy, since both crossing orbitals remain either occupied or unoccupied in the whole range of the coupling constant thanks to a large gap between the occupied and virtual orbitals for all β.

We thus see that the behaviour of the energy lowering ΔE due to the symmetry breaking continuously changes with the deformation of the nuclear framework from

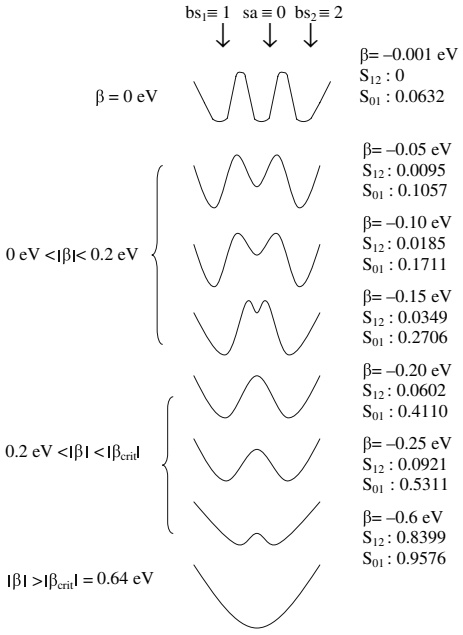

Fig. 7 A schematic representation of the cut of the variational mean-energy hypersurface $E(\Phi)$, Eq. 1, passing through the two degenerate BS solutions (labelled as $bs_1 \equiv 1$ and $bs_2 \equiv 2$) and the SA solution ($sa \equiv 0$) for typical values of the resonance integral β. On the right-hand-side of the figure are listed the values of the overlap integral between the two BS solutions $S_{12} \equiv \langle 1|2\rangle$ and between the BS and SA solution $S_{01} \equiv \langle 1|0\rangle = \langle 2|0\rangle$. See the text for details

the fully symmetric D_{Nh} to the D_{2h} symmetry of the p-models. We see that even the deformed structures very much "mimic" the fully symmetric cyclic polyene, the maximal value of ΔE shifting towards $\beta = 0$ as we approach the fully symmetric structure. Yet, at $\beta = 0$ we must reach the pertinent Kekulé structure. Nonetheless, even for highly deformed structures, we see the tendency of the RHF solutions to simulate that found for cyclic polyenes, a phenomenon we like to refer to as a breaking of an "approximate symmetry". We also note that the critical $|\beta|$ value steadily decreases with the increasing deformation, yet in all cases is much larger than for the actual polyacene: in the case of $N = 14$ structures, we have $\beta_{\text{crit}} = -0.326\,\text{eV}$ for anthracene, $-0.986\,\text{eV}$ for p-anthracene, and $-1.418\,\text{eV}$ for $C_{14}H_{14}$ cyclic polyene (labeled as "ring-$C_{14}H_{14}$" in Fig. 4).

Finally, in Figs. 8 and 9 we present a plot of the bond orders $p_{\mu\nu}$ (i.e., off-diagonal CDWs) for both SA and BS solutions of p-naphatalene and p-anthracene as a function of β. We see that for N=10 in the fully correlated limit ($\beta = 0$), the SA solution converges towards the symmetric Kekulé structure, as in the case of naphthalene, since in this limit there is no distinction between the naphthalene and p-naphthalene Hamiltonians, while the BS solution tends toward the bond order alternating solution. However, as we have seen already, in distinction to naphthalene, whose SA RHF solution is always stable (Corrolary 6.2 and Fig. 2), that of anthracene becomes unstable for $|\beta| < 0.326\,\text{eV}$. The asymmetric bond-order alternating BS solution thus persists even in the highly correlated regime, as for the corresponding cyclic polyene, irrespective of the nuclear framework distorsion. In contrast to the N=10 case, the structure of the SA solution in the fully correlated limit for the anthracenic case may be described

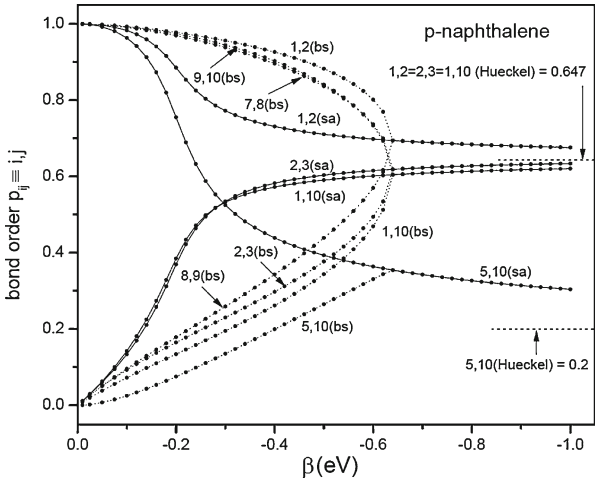

Fig. 8 The dependence of the off-diagonal bond-order matrix elements p_{ij} between the sites i and j for both SA (sa) and BS (bs) RHF solutions of p-naphthalene as a function of the resonance integrals β (in eV). See Fig. 1 for the site-labeling convention employed. On the right hand side, the values of the Hückel model bond-orders are indicated by dashed lines

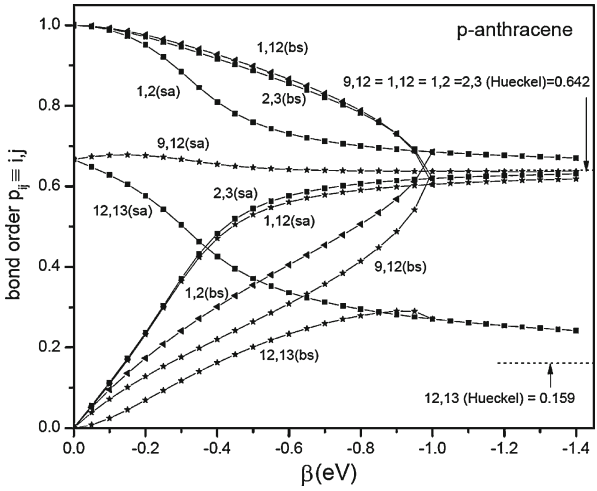

Fig. 9 Same as Fig. 8 for p-anthracene

as that of benzene surrounded by butadienic structures (see Fig. 1f), while the BS solutions display the same bond-length alternating pattern as in the $C_{14}H_{14}$ ring.

Let us finally comment on the existing compounds that are relevant to our π-electron model systems. The fully symmetric $C_{10}H_{10}$ (cyclodecapentaene) forming a regular tengon (all-*cis*[10]annulene) have been actually synthetized in spite of its highly distorted C–C–C angles (144° vs. 120°) and of a serious overcrowding of the inner protons. For these reasons its structure is not planar and seems to involve different *cis–trans* conformers. Yet the barrier between these conformers is low so that the NMR

spectrum implies the equivalence of all CH groups [55], but shows no ring-current effects, presumably due to its nonplanarity [53].

The existence of the di-*trans*-isomer, i.e., our p-naphthalene, seems to be a priory ruled out due to the transannular hydrogen crowding, unless the ring were severely twisted out of plane. However, when the interior hydrogens are replaced with an atom that is linked to the 1,6 positions of the ring (in the numbering of Fig. 1 atoms 5 and 10), crowding can be eliminated. Several such structures involving either methylenic (1,6-methano[10]annulene) or oxygen and nitrogen atoms (1,6-oxido[10]annulene and 1,6-amido[10]annulene, respectively) bridges were synthetized and studied [59] (see also reviews [53–55]). These compounds are not entirely planar, the bridging carbons lying out of plane, but despite the lack of strict planarity there is a significant delocalization of π-electrons. They are characterized by nonalternating "benzenoid" bonds (1.38–1.42 Å), and the distance between the bridging C_1 and C_6 atoms has been estimated to amount to 1.6–2.2 Å, thus excluding the bond across the ring (i.e., the caradiene form), even though the barrier seems to be small. The absence of alternating bond lengths is not surprising, since our models indicate that such an alternation will first occur for much larger cycles.

The structure of the existing [14] annulene corresponds to our p-pyrene. It still involves a serious overcrowding of the inner hydrogens and is likely not entirely planar, yet provides a striking confirmation of the Hückel $(4\nu + 2)$ rule. It is diatropic and exists in two conformations (labelled as *A* and *B*) that differ in the spatial position of inner hydrogens [51]. Conformer *A* forms a crystaline substance and possesses a center of symmetry, which rules out the bond-length alternation.

Similarly as for the 10-membered ring, there has also been synthetized an analogue of our p-anthracene model, namely *syn*- and *anti*-1,6:8,13-bismethano[14]annulene and similar bisoxido compounds [54]. Thus, one requires two out-of-plane bridges across the ring, either on one side (*syn*) or on the opposite sides (*anti*) of the annulene plane, in order to stabilize the p-anthracenic structure. Again, all bonds in this systems were found to be of a similar length ($\sim$1.39 Å) and the perimeter reasonably planar.

7.2 $C_{18}H_{18}$ and $C_{22}H_{22}$ structures

We next briefly present the results for polyenes with 18 and 22 sites that are related to tetracene and pentacene. The energy differences ΔE between the BS and SA RHF solutions, shown in Figs. 10 and 11, respectively, demonstrate that the pattern described in the preceding Sect. 7.1 will repeat itself for larger and larger polyenes, while the critical $|\beta|$ value will steadily increase, reaching and eventually exceeding the spectroscopic value of -2.4 eV. Indeed, for $C_{18}H_{18}$ we observe the same pattern as for the $C_{10}H_{10}$ structures, the RHF solution for tetracene being always singlet stable. Consequently, the ΔE for p-tetracene vanishes at $\beta = 0$, and the two p-benzphenanthrene structures (structures 4 and 5 in Fig. 10), representing "bent" p-tetracene-like structures, behave in a similar way. In contrast, p-coronene and p-perylene, which are more spatially extended and thus closer in their character to the D_{18h} cyclic polyene, behave correspondingly as $\beta \to 0$.

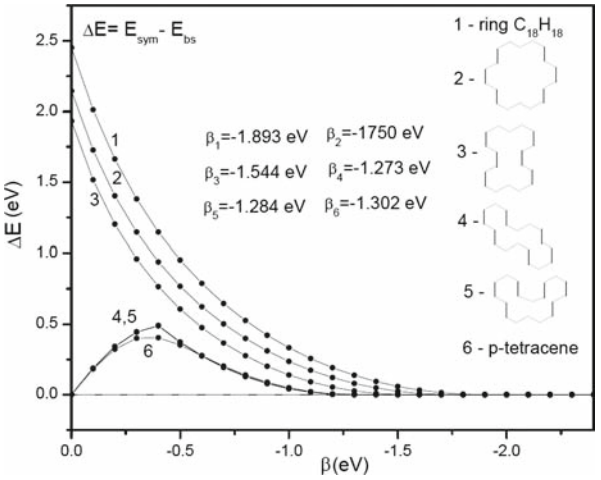

Fig. 10 Same as Fig. 3 for $C_{18}H_{18}$ polyenes

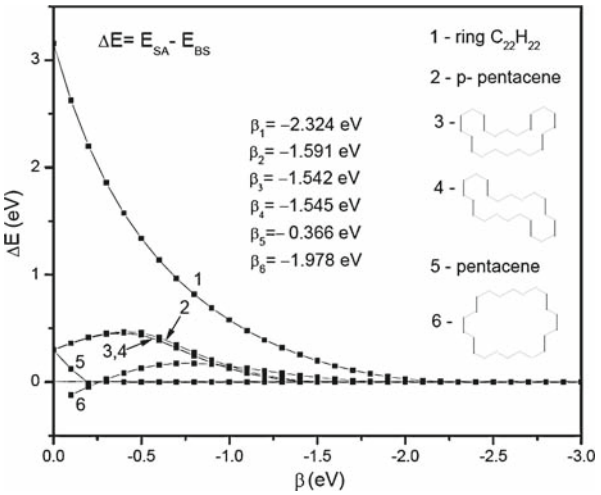

Fig. 11 Same as Fig. 4 for $C_{22}H_{22}$ polyenes

For 22-site polyenes, we again find an analogous situation as for the 14-site anthracenic-type structures. Here, the difference between the critical β values for the D_{22h} cycle and pentacene amounts to almost 2 eV, with β_{crit} for the cycle having an almost spectroscopic value. Again, for $\beta = 0$, the energy difference ΔE for p-pentacene, as well as for other "linear-like" p-pentacene structures (structures 3 and 4 in Fig. 11) is identical with that for pentacene itself. The corresponding SA solution consists of a central benzene surrounded by two butadiene-like structures on each side, while the BS solutions are represented by either of the six Kekulé structures.

An interesting situation arises for the first time for the 18-site polyenes, in which case we can deform the ring structure to an asymmetric p-benzanthracene, having no

(or, rather, C_{1h}) spatial symmetry. Not surprisingly, its RHF solutions are singlet stable in the entire range of the coupling constant, since there is no symmetry to be broken. Yet, as in other cases, the solutions display a CDW along the chain. It is worthwhile to recall, however, that the Hückel solution gives the same bond-order matrix for any of these structures, thus displaying no CDW, all nearest-neighbor bond orders being identical. In other words, at the tight-binding one-electron level of approximation, there is no distinction between various deformed species and the fully symmetric cyclic polyene. This is not the case for the PPP model, which accounts for the two-electron Coulomb interactions, and which leads to BS bond-order alternating solutions for the 18-site ring and its distorted analogues.

We thus consider in greater detail p-benzanthracene, which does not possess any spatial symmetry. This species possesses seven Kekulé structures, three of which have one "cross-bond" (5–18, or 7–16, or 10–15; see Fig. 12), and two having two "cross-bonds" (5–18, 10–15 and 7–16, 10–15). All these structures represent an exact RHF solution for $\beta = 0$, and have the same energy. When we search for the corresponding RHF solutions for $\beta \neq 0$, using the bond-order matrix associated with these Kekulé structures as a starting approximation, we can follow different RHF solutions that correspond to these structures for small enough $|\beta|$ values. The energy of these solutions, obtained by a careful "analytic continuation" with small steps $\Delta\beta$, plotted relative to that having the lowest energy and corresponding to the Kekulé structure 1, are shown in Fig. 12. All these higher energy solutions eventually collapse into the one associated with the first Kekulé structure (structure 1 in Fig. 12). The reason for this behaviour is shown schematically in Fig. 13.

It is instructive to examine the bond-order matrix for the two lowest-energy solutions that are associated with structures 1 and 2 of Fig. 12. These solutions correspond

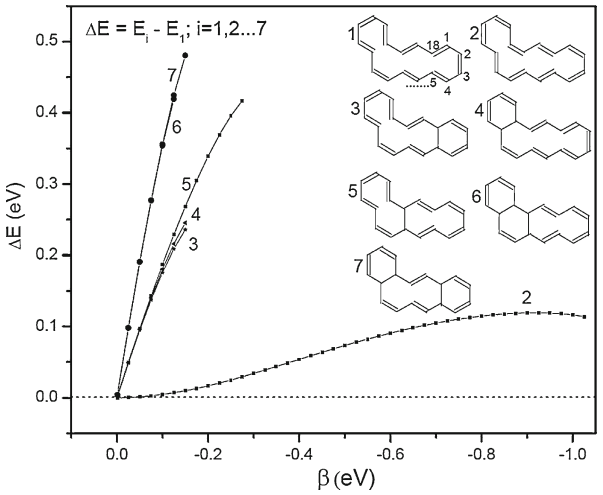

Fig. 12 The energy difference ΔE (in eV) between the energy E_i of the RHF solution that is associated with the Kekulé structure (i) and the energy E_1 of the most stable RHF solution associated with the Kekulé structure 1, $\Delta E = E_i - E_1$, $(i = 1, 2, \ldots, 7)$, of p-benzanthracene, as a function of the resonance integral β (in eV)

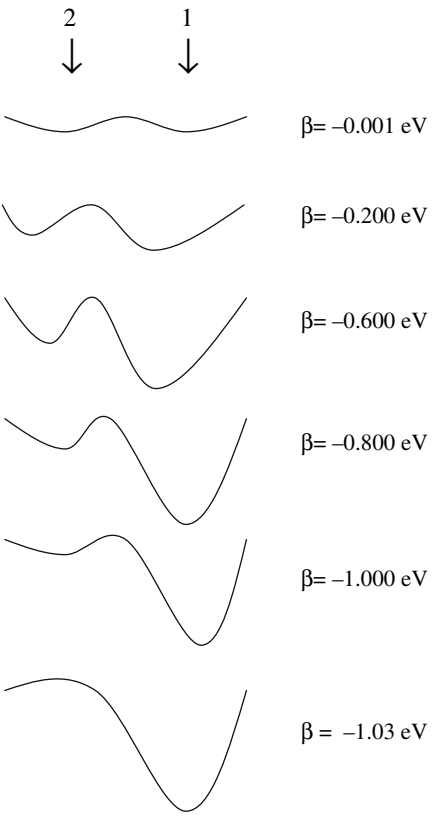

Fig. 13 A schematic representation of the cut of the variational mean-energy hypersurface $E(\Phi)$, Eq. 1, for p-benzanthracene, passing through the RHF solutions associated with the two Kekulé structures 1 and 2 of Fig. 12, for various values of the resonance integral β

to the two degenerate BS solutions for the D_{18h} cyclic polyene that are characterized by alternating bond orders along the chain or, equivalently, by the off-diagonal CDW. Although these solutions are no longer degenerate in the case of p-benzanthracene, they are close in energy when compared with those associated with other Kekulé structures having one or two "cross-bonds" (structures 3–7), respectively). Solutions 1 and 2 also coexist in the largest range of the coupling constant when compared with other solutions, roughly for $0 < |\beta| < 1$ eV, and differ by at most ∼0.1 eV in the energy.

The values of a few typical bond orders as a function of $|\beta|$ for solutions (1) and (2) are given in Table 1. We can measure the strength or amplitude of the associated CDW by comparing the magnitude of neighboring bond orders, i.e., by Δp, where $\Delta p \approx |p_{12} - p_{23}| \approx |p_{23} - p_{34}| \approx \cdots \approx |p_{12,13} - p_{13,14}|$, etc. We see that starting with the maximal bond-order alternation at $\beta = 0$ when $\Delta p = 1$, its intensity weakens as $|\beta|$ increases, Δp becoming ∼0.3 at $\beta = -1$ eV for either solution. The second solution disappears at $\beta \sim -1.029$ eV, and Δp that is associated with the most stable solution then further decreases to ∼0.1 at $\beta = -1.5$ eV, and ∼0.03 at $\beta = -2$ eV. The CDW then practically disappears for $|\beta| > 3$ eV, the bond orders approaching those characterizing the Hückel solution with $\Delta p = 0$ for any $C_{18}H_{18}$ structure (cf. Table 1). This again should be seen from the viewpoint of the D_{18h} cycle, in which

Table 1 Typical bond orders $p_{i,j}$ for the two lowest lying RHF solutions of p-benzanthracene that correspond to the structures 1 and 2 of Fig. 12, for various values of the resonance integral β (in eV)

β	$p_{1,2}$		$p_{2,3}$		$p_{3,4}$		$p_{12,13}$		$p_{13,14}$		$p_{5,18}$		$p_{10,15}$		$p_{7,16}$	
−0.001	0.001	*1.000*	1.000	*0.001*	0.001	*1.000*	1.000	*0.001*	0.001	*1.000*	0.000	*0.000*	0.000	*0.000*	0.000	*0.000*
−0.200	0.173	*0.979*	0.971	*0.160*	0.173	*0.979*	0.971	*0.160*	0.172	*0.979*	0.069	*0.005*	0.068	*0.005*	0.005	*0.004*
−0.400	0.296	*0.944*	0.920	*0.257*	0.296	*0.944*	0.922	*0.258*	0.290	*0.944*	0.158	*0.021*	0.151	*0.025*	0.027	*0.027*
−0.600	0.383	*0.908*	0.869	*0.329*	0.383	*0.908*	0.875	*0.339*	0.371	*0.905*	0.218	*0.047*	0.206	*0.057*	0.063	*0.064*
−0.800	0.448	*0.867*	0.824	*0.394*	0.448	*0.867*	0.835	*0.404*	0.430	*0.860*	0.252	*0.086*	0.237	*0.100*	0.101	*0.112*
−1.000	0.501	*0.808*	0.783	*0.475*	0.502	*0.808*	0.797	*0.494*	0.480	*0.792*	0.267	*0.151*	0.252	*0.166*	0.136	*0.178*
−1.029	0.508	*0.783*	0.776	*0.506*	0.509	*0.784*	0.791	*0.530*	0.487	*0.762*	0.268	*0.180*	0.254	*0.194*	0.140	*0.201*
−1.500	0.603		0.693		0.604		0.708		0.583		0.252		0.245		0.183	
−2.000	0.634		0.661		0.634		0.672		0.620		0.223		0.220		0.176	
−2.500	0.640		0.653		0.641		0.660		0.630		0.207		0.205		0.166	
−3.000	0.642		0.649		0.642		0.655		0.634		0.196		0.195		0.157	
−5.000	0.642		0.645		0.643		0.648		0.638		0.176		0.175		0.140	
Hückel	0.640		0.640		0.640		0.640		0.640		0.145		0.145		0.111	

The site numbering runs consecutively around the cycle as indicated in Fig. 12. The bond orders associated with the higher energy solution 2 that exists only for $|\beta| \leq 1.029$ eV are in italics

case the BS solution exists only for $|\beta| < |\beta_{\text{crit}}| \approx 2\,\text{eV}$, while for D_{2h} p-tetracene, $|\beta_{\text{crit}}| \approx 1.25\,\text{eV}$. Thus, we see a very similar behaviour for p-benzanthracene, in which case no spatial symmetry is present (except, of course, the planarity characterizing all π-electron systems with conjugated double bonds). We like to regard this behaviour as an approximate or induced symmetry breaking.

The cyclooctanonaene ring $C_{18}H_{18}$, referred to as [18]annulene, has the D_{6h} symmetry of our p-coronene, and is perhaps the best studied of all annulenes [51–53]. The overcrowding of the inner hydrogens is not so extreme as to prevent a planar configuration. The X-ray structure suggests that the deviation from the planarity is less than 0.1 Å and seems to exclude the bond-length alternation. There are only slight differences in the peripheral "cisoid" and "transoid" bonds (1.419 vs. 1.382 Å). The molecule is definitely diatropic, and perhaps the most stable of all known annulenes (its decomposition is accelerated by light).

As in previous cases, the p-tetracenic-like structure, namely that of *syn–syn–syn*-1,6:8,17:10:15-trismethano[18]annulene, is also known, as well as other similar bridged structures with various shapes of peripheral π systems [54].

The [22] annulene [53,60] has the structure of our p-ovalene and is again diatropic, the inner protons clearly demonstrating the existence of a magnetically induced diamagnetic ring current, implying aromaticity. Surprisingly, the energy difference ΔE between the BS and SA RHF solutions does not behave as for the ring-$C_{22}H_{22}$, as might be expected, but has a rather small value in the whole range of the existence of the BS solution (Fig. 11, curve 6), even though $|\beta_{\text{crit}}|$ is rather large and close to that of the ring system. Nonetheless, the result is consistent with the fact that no significant bond-length alternation can be expected for realistic β values. We must also note that this system shows a strange behaviour as we approach the fully correlated limit. At $|\beta| \sim 0.5\,\text{eV}$, the SA solution becomes stable again, not unlike in the case of p-naphthalene (Figure 5), and for very small $|\beta|$ values its energy becomes slightly lower than that of the BS solution. The latter is of course characterized by a nearly perfect bond-order alternation, corresponding to one of the Kekulé structures, while the SA one has only 10 ethylenic fragments, trying again for a "benzenoid-like" structure in the center. We must add, however, that both solutions in this limit are associated with very shallow minima and it is very difficult to obtain a proper convergence with a high accuracy.

7.3 Structures with $N > 24$

As the preceding examples of cyclic polyenes C_NH_N with $N = 10, 14, 18$, and 22 indicate, the same pattern will persist for larger and larger cycles and its deformed analogues. As an example, we illustrate this in Figs. 14–16 for $N = 30, 38$, and 42, respectively, for a few typical structures. In Tables 2–5 we present the bond-order matrices for both the SA and BS solutions for the corresponding p-models of $C_{38}H_{38}$ and $C_{42}H_{42}$, respectively. We see again that in the fully correlated $\beta = 0$ limit the SA solution converges to that typical for p-naphthalenic and p-anthracenic structures, representing p-polyacenes with an even and odd number of benzene rings. The bond-order alternation in SA solutions becomes weaker and weaker as we increase the resonance

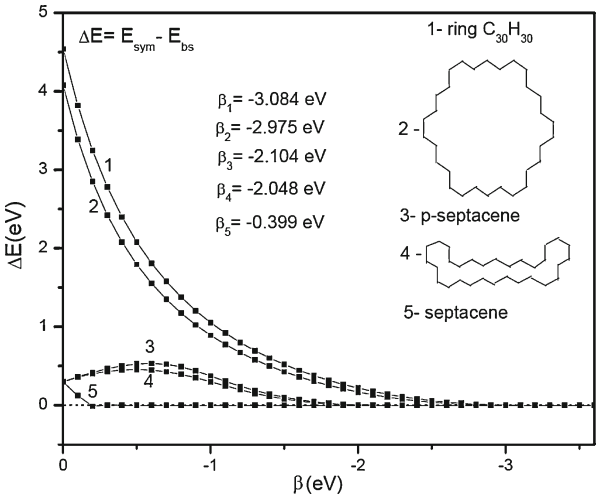

Fig. 14 Same as Fig. 4 for $C_{30}H_{30}$ polyenes

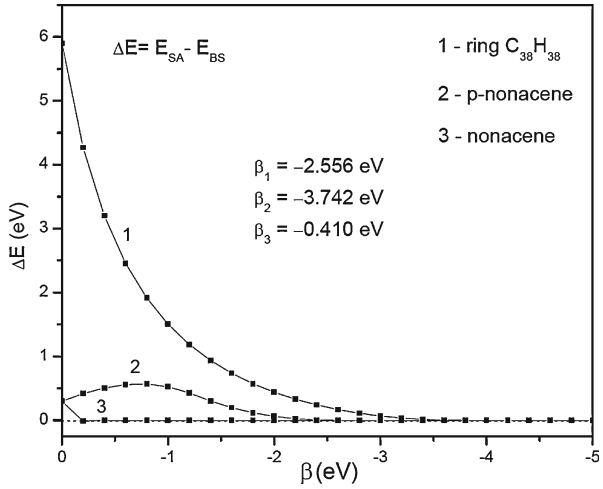

Fig. 15 Same as Fig. 4 for $C_{38}H_{38}$ polyenes

integral $|\beta|$ and, for $|\beta| > |\beta_{\text{crit}}|$ quickly approaches that of the Hückel solution, as may be expected. Yet, for $|\beta| < |\beta_{\text{crit}}|$, where the BS solutions with lower energy exist, the bond-order alternation is significant even for the spectroscopic value of β, implying bond-length alternating structures as in the fully symmetric cyclic polyenes (cf. [31–36]).

The largest known annulene, which is also the least stable of the whole annulenic series, seems to be the [30]annulene [61,62], probably having the structure of p-kekuléne (or p-circumcoronene). Its instability (it almost completely decomposes in 4 hours without protection from daylight) prevented more detailed study or X-ray analysis, as far as we know, but its ultraviolet spectrum has been determined.

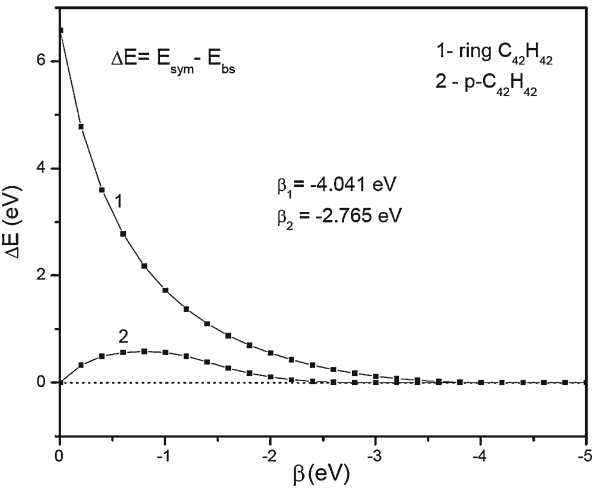

Fig. 16 Same as Fig. 3 for $C_{42}H_{42}$ polyenes

Table 2 Bond orders for the symmetry-adapted (SA) solutions of p-nonacene (p-$C_{38}H_{38}$) for several values of the resonance integral β (in eV) The labeling of bonds is shown in Fig. 17(a)

Bond	β (eV)					
	−3.5	−2.4	−1.5	−1.0	−0.5	−0.001
a	0.636	0.635	0.635	0.653	0.674	0.6667
b	0.636	0.634	0.625	0.526	0.340	0.0014
c	0.636	0.636	0.645	0.763	0.905	1.0000
d	0.635	0.633	0.615	0.446	0.255	0.0008
e	0.636	0.637	0.654	0.815	0.938	1.0000
f	0.634	0.630	0.607	0.419	0.246	0.0008
g	0.638	0.640	0.662	0.825	0.938	1.0000
h	0.632	0.626	0.598	0.425	0.254	0.0008
i	0.650	0.657	0.685	0.821	0.926	1.0000
j	0.637	0.634	0.611	0.457	0.294	0.0012
k	0.172	0.188	0.208	0.125	0.031	0.0001
l	0.123	0.141	0.173	0.144	0.038	0.0003
m	0.106	0.126	0.164	0.223	0.150	0.0008
n	0.100	0.120	0.162	0.311	0.488	0.6667

8 Conclusions

In this work we explored the propagation of the space-symmetry breaking effects at the RHF level of approximation when proceeding from the highly symmetric structures to those of lower symmetry, or no symmetry at all, using the PPP model of cyclic polyenes C_NH_N with a nondegenerate ground state ($N = 2n = 4\nu + 2,\ \nu = 1, 2, 3, \ldots$). Thus, we start with the most symmetric cyclic polyene C_NH_N, whose sites are located at the vertices of a regular N-gon (which we refer to as "ring-polyenes" or rings), and

Table 3 Bond orders for the broken-symmetry (BS) solutions of p-nonacene (p-$C_{38}H_{38}$) for several values of the resonance integral β (in eV) in the range of singlet instability ($\beta_{crit} = -2.556$ eV)

Bond		β (eV)									
		−2.4		−1.5		−1.0		−0.5		−.001	
a	A	0.709	0.558	0.828	0.423	0.880	0.351	0.942	0.241	1.0000	0.0008
b	B	0.559	0.708	0.423	0.827	0.352	0.880	0.241	0.942	0.0008	1.0000
c	C	0.707	0.562	0.826	0.426	0.879	0.352	0.942	0.242	1.0000	0.0008
d	D	0.562	0.702	0.427	0.821	0.353	0.877	0.242	0.942	0.0008	1.0000
e	E	0.702	0.569	0.819	0.435	0.876	0.358	0.942	0.242	1.0000	0.0008
f	F	0.569	0.692	0.438	0.804	0.359	0.865	0.243	0.940	0.0008	1.0000
g	G	0.695	0.582	0.805	0.461	0.866	0.380	0.939	0.250	1.0000	0.0008
h	H	0.576	0.675	0.458	0.762	0.378	0.817	0.252	0.907	0.0008	1.0000
i	I	0.700	0.613	0.794	0.529	0.851	0.470	0.927	0.341	1.0000	0.0010
j	J	0.589	0.677	0.468	0.755	0.415	0.806	0.293	0.895	0.0010	1.0000
k	K	0.151	0.216	0.088	0.257	0.058	0.257	0.024	0.190	0.0000	0.0000
l	L	0.110	0.155	0.047	0.144	0.022	0.108	0.005	0.040	0.0000	0.0000
m	M	0.099	0.127	0.035	0.083	0.011	0.045	0.001	0.008	0.0000	0.0000
n	N	0.101	0.110	0.036	0.051	0.011	0.020	0.0005	0.002	0.0000	0.0000

The labeling of bonds is shown in Fig. 17(a)

whose RHF (or, in fact, a general minimum basis set IPM) solution is fully determined by the D_{Nh} symmetry of the model. We then systematically deform this highly symmetric framework while preserving the constant C–C internuclear separations and, in most cases, consider the systems with the standard C–C–C angles of $2\pi/3$. In this way we reach various "perimeter" models of standard aromatic hydrocarbons. All these systems may be regarded as models of linear polyenes with Born–von Kármán boundary conditions. The properties of the ring polyenes were studied in detail earlier, both at the RHF and post-HF correlated levels [10,11,13,15,31–36,49,50]. Their SA RHF solutions become singlet unstable for sufficiently large coupling constants (or small enough resonance integrals $|\beta|$), implying the existence of BS RHF solutions of different types. Those having the lowest energy and corresponding to the absolute minimum on the mean-energy, variational hypersurface are those BS solutions that possess the D_{nh} symmetry and are characterized by the CDW represented by alternating bond orders along the chain. An analogous phenomenon is found at the ab initio level, in particular when considering chains of hydrogen atoms [17], but for long polyenic chains as well.

The BS solutions just mentioned imply the tendency towards the actual distortion of the nuclear framework, namely a distortion that no longer preserves the identical C–C bond lengths, thus leading to structures with alternating bond-lengths along the chain (cf. Ref. [31]). Indeed, it can be shown (cf., e.g., [6]) that such a distortion of the nuclear framework that is "in-phase" with the CDW of one of the degenerate BS solutions invariably lowers its energy, while the distortion that is "out-of-phase" with the CDW increases the energy (in each case with a nonzero first derivative of

Table 4 Bond orders for the symmetry-adapted (SA) solutions of p-decacene (p-$C_{42}H_{42}$) for several values of the resonance integral β (in eV)

Bond	β (eV)					
	−3.5	−2.4	−1.5	−1.0	−0.5	−0.001
a	0.6356	0.6345	0.6288	0.5798	0.4637	0.0011
b	0.6354	0.6350	0.6430	0.7245	0.8415	1.0000
c	0.6356	0.6338	0.6149	0.4596	0.2744	0.0008
d	0.6353	0.6357	0.6557	0.8130	0.9315	1.0000
e	0.6354	0.6326	0.6035	0.4048	0.2460	0.0008
f	0.6356	0.6369	0.6652	0.8438	0.9410	1.0000
g	0.6345	0.6305	0.5952	0.3919	0.2440	0.0008
h	0.6373	0.6401	0.6723	0.8435	0.9385	1.0000
i	0.6316	0.6255	0.5883	0.4043	0.2527	0.0008
j	0.6493	0.6572	0.6931	0.8348	0.9270	1.0000
k	0.6373	0.6335	0.6028	0.4382	0.2934	0.0011
l	0.1721	0.1876	0.2022	0.0985	0.0268	0.0000
m	0.1222	0.1407	0.1698	0.1015	0.0190	0.0000
n	0.1044	0.1241	0.1638	0.1676	0.0686	0.0000
o	0.0968	0.1172	0.1637	0.2783	0.2820	0.0000
p	0.0947	0.1152	0.1642	0.3443	0.6053	1.0000

The labeling of bonds is shown in Fig. 17(b)

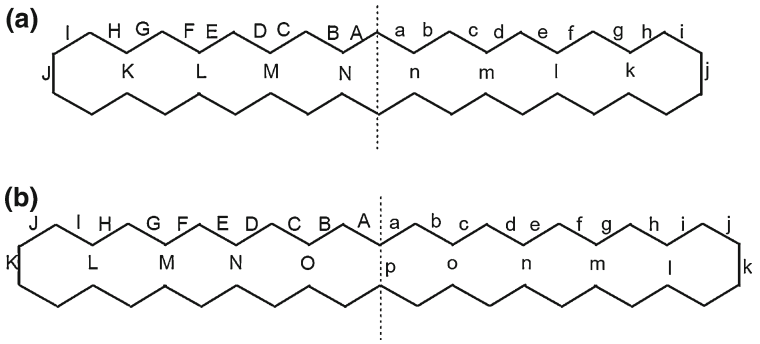

Fig. 17 The labelling of bonds in $C_{38}H_{38}$ and $C_{42}H_{42}$ polyenes used in Tables 2, 3–5, respectively

the corresponding potential, so that both potential energy curves cross with a finite angle among them). However, the latter solution exists only in the limited region of distortions, while the in-phase distorted one reaches eventually its minimum at some finite distortion (as measured, e.g., by the difference between the longer and shorter bond lengths), implying the most stable structure at the RHF or IPM level. In the case of cyclic polyenes, the preference for a bond-length alternating structure persists even at the post-HF correlated level (see above given references). Needless to say that

Table 5 Bond orders for the broken-symmetry (BS) solutions of p-decacene (p-$C_{42}H_{42}$) for several values of the resonance integral β (in eV) in the range of singlet instability ($\beta_{crit} = -2.765$ eV)

Bond		β (eV)									
		−2.4		−1.5		−1.0		−0.5		−0.001	
a	A	0.5279	0.7381	0.4192	0.8312	0.3509	0.8803	0.2414	0.9425	0.0008	1.0000
b	B	0.7374	0.5289	0.8308	0.4197	0.8802	0.3510	0.9425	0.2414	1.0000	0.0008
c	C	0.5304	0.7350	0.4207	0.8293	0.3513	0.8798	0.2414	0.9424	0.0008	1.0000
d	D	0.7332	0.5337	0.8281	0.4231	0.8795	0.3521	0.9424	0.2415	1.0000	0.0008
e	E	0.5363	0.7276	0.4253	0.8230	0.3530	0.8773	0.2416	0.9422	0.0008	1.0000
f	F	0.7256	0.5435	0.8212	0.4332	0.8763	0.3573	0.9421	0.2421	1.0000	0.0008
g	G	0.5455	0.7141	0.4360	0.8057	0.3591	0.8654	0.2427	0.9398	0.0008	1.0000
h	H	0.7155	0.5602	0.8065	0.4594	0.8654	0.3799	0.9390	0.2500	1.0000	0.0008
i	I	0.5563	0.6927	0.4566	0.7640	0.3782	0.8172	0.2518	0.9068	0.0008	1.0000
j	J	0.7160	0.5951	0.7953	0.5272	0.8512	0.4696	0.9273	0.3404	1.0000	0.0011
k	K	0.5717	0.6931	0.4847	0.7569	0.4144	0.8058	0.2926	0.8948	0.0011	1.0000
l	L	0.1341	0.2241	0.0856	0.2570	0.0581	0.2566	0.0237	0.1898	0.0000	0.0000
m	M	0.0912	0.1559	0.0431	0.1431	0.0215	0.1079	0.0045	0.0398	0.0000	0.0000
n	N	0.0787	0.1204	0.0282	0.0812	0.0096	0.0447	0.0009	0.0082	0.0000	0.0000
o	O	0.0775	0.0978	0.0248	0.0475	0.0065	0.0188	0.0003	0.0017	0.0000	0.0000
p		0.0840		0.0307		0.0089		0.0004		0.0000	

The labeling of bonds is shown in Fig. 17(b)

when $N \to \infty$, the critical value $|\beta_{\text{crit}}|$ of the resonance or hopping integral increases correspondingly, reaching its physical (or spectroscopic) value already at $N \sim 26$ or 30.

It should be noted that this phenomenon is in fact analogous to the formation of the Wigner lattice in the case of a low-density electron gas. Qualitatively, this tendency is easy to understand when we consider a chain of hydrogen atoms in a D_{Nh} arrangement and instead of the resonance integral β we vary the H–H internuclear separation $R_{\text{H–H}}$. Clearly, when $R_{\text{H–H}}$ exceeds the H_2 equilibrium bond length, the system will have a tendency to break the D_{Nh} symmetry to that of D_{nh}, since in the $R_{\text{H–H}} \to \infty$ limit, the energy difference between the D_{Nh} and D_{nh} solutions will amount to nD_e, where D_e designates the dissociation energy of H_2 [17].

As already stated, the main objective of our study was to explore the symmetry breaking phenomenon for real and hypothetical systems possessing different spatial symmetry, yet identical in their composition. For this purpose we gradually distorted the D_{Nh} cyclic polyenes, reaching eventually the "perimeter models" (or p-models) of various aromatic hydrocarbons having the same number of carbon atomic sites. In this way we lowered the D_{Nh} structures to those with the D_{6h}, D_{2h} or, if possible, C_{1h} symmetry. A comparison was also made with the corresponding aromatic hydrocarbons studied earlier [13].

Although, generally, the lowering of the symmetry of the nuclear framework brings about the lowering of the critical value $|\beta_{\text{crit}}|$ of the resonance integral, and thus restricts the interval of β values in which the RHF solution is singlet unstable, the symmetry breaking phenomenon persists as long as some symmetry remains to be broken. This lowering of $|\beta_{\text{crit}}|$ is particularly severe for the corresponding linear polyacenes (see Fig. 2), in which case the SA RHF solution is singlet unstable only for those polyacenes having an odd number of benzene rings [13]. Since at the PPP level of approximation the p-models of polyacenes (i.e., p-polyacenes) in the fully correlated limit represent identical systems as polyacenes themselves, we can draw on the earlier formulated theorems [13] concerning the structure and degeneracy of RHF solutions in this limit, as given by the VB structures. We also note here that at the Hückel level of approximation there is no distinction between various cyclic-polyene species as long as they involve the same number of sites.

We thus find that for the structures having an even number of benzene rings in the corresponding polyacene, namely those with even ν, the energy difference between the BS and SA solutions tends toward zero in view of the inherent stability of polyacenes with an even number of benzene rings. In view of this fact, the p-model solutions become again stable in the vicinity of the fully correlated limit (see Fig. 5). This is not the case for less-distorted structures, which are closer in their geometry to the N-gonic structures, and thus do not have Kekulé-type VB structures with bonds across the "cycle" (see Figs. 3, 10, and 16). In contrast, for the structures with odd ν, in which case the polyacene solutions are singlet unstable (although their $|\beta_{\text{crit}}|$ is much smaller), the energy difference ΔE between the SA and BS solutions tends towards the same finite value as $\beta \to 0$, given by the difference between the energies of benzene and three ethylenic fragments, since in view of the nonexistence of a symmetric Kekulé structure the SA solution in this limit consists of a central benzenic ring surrounded by ethylenic fragments [as illustrated for the $\nu = 3$ case in Fig. 1f; cf. also Figs. 8 and

9, and Tables 2 and 4]. Note that in all cases, the ΔE value for $\beta = 0$ is the same, regardless of the value of N [$\Delta E(\beta = 0) \approx 0.3\,\mathrm{eV}$].

Needless to say that in all cases when the distorted system possesses some nontrivial symmetry (e.g., D_{2h} or D_{6h}), the BS solutions are again degenerate and belong to an appropriately lower symmetry (C_{1h} or D_{3h}, respectively; clearly symmetry implied by the planarity of these systems cannot be broken for the semiempirical models employed). In this regard an interesting case arises once the distortion eliminates all the spatial symmetry, as in the case of p-benzanthracene ($N = 18$, Fig. 12). Although all the RHF solutions remain stable in the whole range of the coupling constant, as may have been expected, we nonetheless observe—at least in the vicinity of the fully correlated limit—the existence of quasidegenerate solutions associated with the standard (i.e., without any "cross-links") Kekulé structures with alternating bond orders along the chain. This is the most frapant case of the phenomenon that we refer to as the breaking of an approximate symmetry or an implied symmetry breaking.

As outlined in the preceding section, a number of seemingly hypothetical structures does actually exist and has been studied experimentally. The most surprising are the p-models of linear polyacenes, which are made almost planar thanks to the stabilizing out-of-plane bridges. Even these systems nicely conform to the Hückel $(4\nu + 2)$ rule and show a definite "aromatic" character (cf. [53]). This also conforms with our results, since for these systems $|\beta_{\mathrm{crit}}|$ is still much smaller than its spectroscopic value, so that no bond-length alternation can be expected. In any case, the energy lowering due to the symmetry breaking bond-length alternation (as implied by the CDW of the respective RHF solutions) is much smaller than for more "circular" structures that are closer to the standard annulenes.

Of course, for sufficiently large polyenes, the bond-length alternation will arise, the extreme case being represented by polyacetylene. In fact, we can expect that for rings with more than 30 carbon sites the bond-length alternation will set in. However, such rings are very difficult to study experimentally due to their inherent instability (cf. ref. [61,62]). Once, however, $N \to \infty$, our models describe polyacetylene (with Born–von Kármán boundary conditions) irrespective of which stereoisomer is considered, and computed bond-length alternation ($\sim$0.05 Å) is born out by experiment (cf. [6] and references therein).

Finally, let us also emphasize the commonality of the behavior shown by various stereoisomers of cyclic polyenes, implying the usefulness of a highly symmetrical D_{Nh} model, which enables a huge simplification of quantum-mechanical calculations at any level of approximation. In fact, at the Hubbard Hamiltonian level one can easily generate the exact results by solving Lieb-Wu equations, not to mention of course that for the Hückel Hamiltonian there is no difference between various stereoisomers. In any case, many of the properties of these systems found for the most symmetric structures propagate to isomers that possess much lower or no symmetry.

In summary, our study of cyclic polyenes in their various geometric arrangements clearly indicates not only the potential richness of various BS RHF solutions, but also their connection with those arising from highly-symmetrical structures, as well as with those encountered in the highly correlated limit. These relationships remind us the role played by Welsh diagrams in molecular spectroscopy.

Acknowledgments Continued support by NSERC (J.P.) is gratefully acknowledged. We would also like to thank to Ms. Laura Thompson for carrying out the initial test calculations.

References

1. J. Paldus, in *Theory and Applications of Computational Chemistry: The First Forty Years*, eds. by C.F. Dykstra, G. Frenking, K.S. Kim, G.E. Scuseria), Chap. 7 (Elsevier, Amsterdam, 2005) pp. 115–147
2. C. Froese-Fischer, *The Hartree-Fock Method for Atoms: A Numerical Approach* (Wiley, New York 1977)
3. K. Kowalski, K. Jankowski, Phys. Rev. Lett. **81**, 1195 (1998)
4. P.-O. Löwdin, Rev. Mod. Phys. **35**, 496 (1963)
5. H. Fukutome, Int. J. Quant. Chem. **20**, 955 (1981)
6. J. Paldus, in *Self-Consistent Field: Theory and Applications*, eds. by R. Carbó, M. Klobukowski (Elsevier, Amsterdam, 1990) pp. 1–45
7. J.L. Stuber, J. Paldus, in *Fundamental World of Quantum Chemistry*, eds. by R.J. Brändas, E.S. Kryachko, vol. I (Kluwer, Dordrecht, 2003) pp. 67–139
8. J. Koutecký, J. Chem. Phys. **46**, 2443 (1967)
9. D.J. Thouless, *The Quantum Mechanics of Many-Body Systems* (Academic, New York, 1961)
10. J. Čížek, J. Paldus, J. Chem. Phys. **47**, 3976 (1967)
11. J. Paldus, J. Čížek, J. Polymer Sci. C **29**, 199 (1970)
12. J. Koutecký, J. Paldus, J. Čížek, J. Chem. Phys. **83**, 1722 (1985)
13. J. Čížek, J. Paldus, J. Chem. Phys. **53**, 821 (1970)
14. J. Paldus, J. Čížek, Phys. Rev. A **2**, 2268 (1970)
15. J. Čížek, J. Paldus, Phys. Rev. A **3**, 525 (1971)
16. M. Bénard, J. Chem. Phys. **71**, 2546 (1979)
17. M. Bénard, J. Paldus, J. Chem. Phys. **72**, 6546 (1980)
18. J. Paldus, J. Čížek, Can. J. Chem. **63**, 1803 (1985)
19. M. Bénard, W.G. Laidlaw, J. Paldus, Can. J. Chem. **63**, 1797 (1985)
20. M. Bénard, W.G. Laidlaw, J. Paldus, Chem. Phys. **103**, 43 (1986)
21. J. Paldus, J. Čížek, Chem. Phys. Lett. **3**, 1 (1969)
22. J. Paldus, J. Čížek, J. Chem. Phys. **52**, 2919 (1970)
23. J. Paldus, J. Čížek, J. Chem. Phys. **54**, 2293 (1971)
24. J. Paldus, A. Veillard, Chem. Phys. Lett. **50**, 6 (1977)
25. J. Paldus, A. Veillard, Mol. Phys. **35**, 445 (1978)
26. J. Paldus, J. Čížek, B.A. Keating, Phys. Rev. A **8**, 640 (1973)
27. R.G. Parr, *The Quantum Theory of Molecular Electronic Structure* (Benjamin, New York, 1963)
28. C.C.J. Roothaan, Rev. Mod. Phys. **25**, 69 (1951)
29. E.R. Davidson, W.T. Borden, J. Phys. Chem. **87**, 4783 (1983)
30. W.D. Allen, D.A. Horner, R.L. Dekock, R.B. Remington, H.F. Schaefer III, Chem. Phys. **133**, 11 (1989)
31. J. Paldus, E. Chin, Intern. J. Quant. Chem. **24**, 373 (1983)
32. J. Paldus, E. Chin, M.G. Grey, Intern. J. Quant. Chem. **24**, 395 (1983)
33. R. Pauncz, J. Paldus, Intern. J. Quant. Chem. **24**, 411 (1983)
34. J. Paldus, M. Takahashi, Intern. J. Quant. Chem. **25**, 423 (1984)
35. M. Takahashi, J. Paldus, Intern. J. Quant. Chem. **26**, 349 (1984)
36. M. Takahashi, J. Paldus, Intern. J. Quant. Chem. **28**, 459 (1985)
37. L.A. Barnes, R. Lindh, Chem. Phys. Lett. **223**, 207 (1994)
38. K.R. Asmis, T.R. Taylor, D.M. Neumark, J. Chem. Phys. **111**, 8838 (1999)
39. S.R. Gwaltney, M. Head-Gordon, Phys. Chem. Chem. Phys. **3**, 4495 (2001)
40. X. Li, J. Paldus, J. Chem. Phys. **126**, 224304 (2007)
41. F. Holka, P. Neogrády, M. Urban, J. Paldus, Coll. Czech. Chem. Commun. **72**, 197 (2007)
42. J. Paldus, in *Theoretical Chemistry: Advances and Perspectives*, eds. by E. Eyring, D.J. Henderson, vol. 2 (Academic, New York, 1975) pp. 131–290
43. N. Mataga, K. Nishimoto, Z. Phys. Chem. (Frankfurt) **13**, 140 (1957)
44. M. Goeppert-Mayer, A.L. Sklar, J. Chem. Phys. **6**, 635 (1938)
45. E.H. Lieb, F.Y. Wu, Phys. Rev. Lett. **20**, 1445 (1968)
46. K. Hashimoto, J. Čížek, J. Paldus, Intern. J. Quant. Chem. **34**, 407 (1988)

47. J. Čížek, K. Hashimoto, J. Paldus, M. Takahashi, Israel J. Chem. **31**, 423 (1991)
48. J. Paldus, J. Čížek, Prog. Theor. Phys. (Kyoto) **42**, 769 (1969)
49. J. Paldus, M. Takahashi, R.W.H. Cho, Phys. Rev. B **30**, 4267 (1984)
50. M. Takahashi, J. Paldus, Phys. Rev. B **31**, 5152 (1985)
51. F. Sondheimer, Proc. R. Soc. London A **297**, 173 (1967)
52. F. Sondheimer, Acc. Chem. Res. **5**, 81 (1972)
53. F. Sondheimer, Chimia **28**, 163 (1974)
54. P.J. Gerratt, *Aromaticity* (Wiley, New York, 1986)
55. D. Lloyd, *The Chemistry of Conjugated Cyclic Compounds. To Be or Not To Be Like Benzene?* (Wiley, New York, 1989)
56. H. Fukutome, Prog. Theor. Phys. (Kyoto) **40**, 998–1227 (1968)
57. R.A. Harris, L.M. Falicov, J. Chem. Phys. **51**, 5034 (1969) and references therein
58. D. Cazes, L. Salem, C. Tric, J. Polym. Sci. C **29**, 494 (1974)
59. E. Vogel, H.D. Roth, Angew. Chem. Int. Ed. **3**, 228 (1964)
60. R.M. McQuilkin, B.W. Metcalf, F. Sondheimer, Chem. Commun, 338 (1971)
61. F. Sondheimer, R. Wolovsky, Y. Amiel, J. Am. Chem. Soc. **84**, 274 (1962)
62. F. Sondheimer, Y. Gaoni, J. Am. Chem. Soc. **84**, 3520 (1962)